The definitive publisher version is available online at https://doi.org/10.1016/j.jwpe.2022.102627

Sorptive removal of ibuprofen from water by natural porous biochar derived from recyclable plane tree leaf waste

Xu Yang[a,b], Xinbo Zhang[a,b,*], Huu Hao Ngo[c,a,*], Wenshan Guo[c,a],,Jiangbo Huo[a,b], Qing Du[a,b], Yufeng Zhang[a,b], Chaocan Li[a,b], Fei Yang[a,b]

[a]*Joint Research Centre for Protective Infrastructure Technology and Environmental Green Bioprocess, School of Environmental and Municipal Engineering, Tianjin Chengjian University, Tianjin 300384, China*

[b]*Tianjin Key Laboratory of Aquatic Science and Technology, Tianjin Chengjian University, Jinjing Road 26, Tianjin 300384, China*

[c]*Centre for Technology in Water and Wastewater, School of Civil and Environmental Engineering, University of Technology Sydney, Sydney, NSW 2007, Australia*

*Correspondence authors: Email: zxbcj2006@126.com (X. B. Zhang);

ngohuuhao121@gmail.com (H. H. Ngo)

Abstract

To remove ibuprofen (IBP) in water efficiently and economically, plane tree leaf-derived biochar (P-BC) as a new adsorbent was prepared via pyrolysis at 600 ℃. Textural characterizations of P-BC exhibited a porous structure and abundant hydroxyl groups. The results of FTIR and XPS indicated that -OH functional groups played a key role in the adsorption process. Batch adsorption studies were carried out at pH values of 2 to 8, adsorbent dosage of 0.1 to 2.0 g/L and initial concentrations of 500 to 5000 μg/L. Adsorption results showed that P-BC (1.0 g/L) could remove as much as 96.34% of ibuprofen (2000μg/L) in a strong acidic environment (*i.e*. pH 2). The adsorption of ibuprofen by P-BC was found to be more consistent with the pseudo-second order kinetic model and Langmuir isothermal model with higher correlation coefficients of 0.999 and 0.996, respectively. Its maximum adsorption capacity was up to 10410 μg/g. A mechanism analysis demonstrated that the -OH functional groups on the surface of P-BC could form hydrogen bonds with IBP as donors and acceptors, respectively. It played a predominant role in removing IBP. In particular the fabricated P-BC is an effective and recyclable sorbent and its efficiency in removing ibuprofen can still reach more than 70% after five regenerations. The total production cost of P-BC is 4.05 USD / kg, which is equivalent to the treatment cost of only 0.004 USD/L wastewater. The results revealed that P-BC is an environment-friendly, low-cost and efficient adsorbent for removing IBP from water.

Key words： Biochar; Hydrogen bonding; Ibuprofen; Plane tree leaf; Regeneration

1. INTRODUCTION

Pharmaceuticals and personal care products (PPCPs), including antibiotic, painkillers, hair dyes, antiseptics and so on, have been widely used in agriculture, industry, medicine and people's daily necessities [1]. With the increasing consumption of PPCPs, it is difficult to efficiently remove PPCPs from wastewater by conventional wastewater treatment processes, resulting in the release of large amounts of untreated PPCPs into the environment. This consequently poses a potential threat to the natural environment and human health [2,3].

Ibuprofen (IBP), one of the world's most widely consumed nonsteroidal anti-inflammatory drugs among PPCPs, is commonly used to relieve symptoms of arthritis, pain and fever. It also exhibits a state of "pseudo-persistence" in water due to its relative stability and hydrophilicity [4]. It is also the most common drug detected in water bodies and can even reach the mg/L level in the case of pharmaceutical industry wastewater [5,6]. It has been reported that IBP can alter the cardiac physiology and hemodynamics of embryos, impair cardiovascular development in zebrafish, reduce the reproductive rate of crustaceans, and possibly induce compensatory hypogonadism in males [7-9]. For these reasons, removing IBP from water is of great importance for maintaining the good health of the environment and people.

In the past few decades, more and more technologies have been invented to remove IBP from water, including constructed wetland, biodegradation, photocatalysis, ozone oxidation, and adsorption [10-14]. Among the currently available methods, adsorption is one of the most promising strategies for trace IBP retention [15]. Activated carbon, clay and carbon nanotubes have been used to adsorb IBP from water [16-18]. Generally, the preparation of carbon

nanomaterials requires chemical reaction steps and produced nanomaterial further requires purification steps. Therefore, it is necessary to find an alternative adsorbent material that can be simply prepared without any chemical modification [19].

Biochar is a kind of high carbon content solid product obtained by pyrolysis of biomass materials (such as plant straw, municipal sludge, etc.) under limited oxygen conditions. It has the advantages of helping save the environment, low cost, high efficiency, and a lot of potential in terms of environment pollutants removal due to the characteristics of high specific surface area, abundant functional groups [20]. Over the past couple of years, various biochars have been reported to use for removing IBP from wastewater. Essandoh et al. [21] reported that the adsorption capacity of pine wood biochar prepared at 425 °C for IBP in water was 10.74mg/g under the conditions of pH3 and a dosage of 4g/L. Mondal et al. [22] treated mung bean shell biochar by steam activation, and the maximum adsorption capacity of IBP in water was 59.76mg/g at pH2 and a dosage of 0.1g/L. In another study, Chakraborty et al. [23] also carried out steam activation treatment on wood apple shell biochar. It was found that the removal rate of IBP in water by biochar increased from 82% to 85.5% with the adsorption capacity of 12.658 mg/g. Moreover, Show et al. [23] investigated the adsorption effect of IBP by acid-base modification of terminalia katappa shell biochar. The results exhibited the alkali modified biochar processed better adsorption capacity of IBP of 9.52mg/g. Among them, mung bean husk biochar and wood apple biochar used steam to be activated in the preparation process, and terminalia katappa shell biochar was prepared by acid and alkali treatments. Therefore, these additional steps not only complicated the preparation process, but also increased the production

cost of biochar. Furthermore, the effect of coexisting ions on IBP adsorption by biochar needs to be explored due to various ions in the actual wastewater, which may effect on the adsorption performance of the adsorbent. Consequently, the novel green biochar need to be further explored with simple preparation process, cost-effective, high efficiency and ion interference resistance, so as to be more potential for practical applications.

Nowadays, green landscaping waste (such as fallen leaves, tree pruning, etc.) is mainly disposed of by composting, burning or landfill, which not only pollutes the environment, but also increases the burden of garbage treatment plants. Therefore, the proper disposal and resource-based utilization of green landscaping waste has become a fairly widespread concern [25,26]. Kim et al. [19] examined maple leaf-derived biochar as a sorbent in IBP elimination from aqueous medium. They found that the adsorption capacity of maple leaf-derived biochar prepared at 750 °C for tetracycline in water was as high as 407.3 mg/g due to metal complexation, hydrogen bonding and hydrophobic interactions. Therefore, using landscaping waste to prepare biochar and remove pollutants from water is a "win-win" solution.

In this study a biochar was prepared to remove IBP from water through resource utilization of plane tree fallen leaves. The surface structure, composition and functional groups of biochar before and after IBP adsorption were characterized. In addition, the influencing factors and mechanism for removing IBP from water by plane tree leaf-derived biochar were investigated and explored, and the reuse of biochar was evaluated experimentally. Finally, the economic evaluation and safe disposal of P-BC were discussed to improve its applicability. It provides theoretical and data support for the practical removal of IBP in water by P-BC. This

investigation can pave the way for better resource utilization of biomass, and a low-cost and green adsorbent for IBP from water.

2. MATERIALS AND METHODS

2.1. Materials and chemicals

The raw materials for biochar were sourced from the fallen leaves of French plane trees grown by the landscaping of Tianjin Chengjian University (Tianjin, China). IBP (ibuprofen) was purchased from Beijing Solarbio Technology Co., Ltd (Beijing, China). Methanol was obtained from Thermo Fisher Scientific (USA). Absolute ethanol and glacial acetic acid were obtained from Shanghai Macklin Biochemical Share Co., Ltd (Shanghai, China). NaCl, $NaNO_3$, Na_2SO_4 and Na_3PO_4 used in the experiment were obtained from Tianjin Damao Chemical Reagent Factory (Tianjin, China). All chemicals or reagents used are of analytical purity or higher purity.

2.2. Preparation of biochar

The preparation method of biochar has changed to some extent in the preparation methods of Kim et al [19] and Zhang et al. [27]. In general, the collected fallen leaves from the plane tree were washed with distilled water, and then dried in an oven at 70 °C until constant weight was achieved. The oven dried materials were sieved (50 mesh) after crushing. Appropriate amounts of leaf powder were taken and placed in a crucible, sealed with aluminum foil paper and placed in a muffle furnace, with a heating rate of 5 °C/min, reaching a final temperature of 600 °C and a residence time of 2 h. Following this the biochar was cooled to room temperature and passed through a 100-mesh sieve. Then it was washed several times with deionized water,

130 dried and sealed for storage, and given the name P-BC.

131 *2.3. Characterization of biochar*

132 Scanning electron microscopy (SEM) (Regulus 8100, Japan) was conducted to observe
133 the morphology and structure of P-BC. The surface functional groups of P-BC were identified
134 using Fourier Transform infrared spectroscopy (FTIR) (NiciletiS10, USA) at 400 to 4000 cm^{-1}
135 with 32 scans being taken at a 4 cm^{-1} resolution. After vacuum degassing at 573.15 K for 4 h,
136 specific surface area and pore volume of P-BC were measured by N_2 adsorption/desorption
137 isotherms using a specific surface area and porosity analyzer (TristarII3020, USA) at 77 K.
138 After heating P-BC at 800 °C for 4 h, the ash content was determined by calculating the mass
139 loss before and after. The carbon, hydrogen and nitrogen contents of biochar were determined
140 using an elemental analyzer (Vario EL cube, Germany) while the oxygen content was calculated
141 from mass conservation. The surface composition of P-BC before and after IBP adsorption was
142 performed by X-ray photoelectron spectroscopy (XPS, K-alpha, UK). The zeta potential of
143 biochar at different pH levels was measured by Zeta potential analyzer (Zetasizer Nano ZS,
144 Malvern, UK).

145 *2.4. Batch experiments of IBP adsorption*

146 IBP stock solution (20 mg/L) was prepared by dissolving IBP in ultrapure water. P-BC
147 (0.1 g) was added to the IBP solution (100 mL) in a 250 mL conical flask. IBP concentration
148 was determined by sampling after 24 h oscillation on a 150 rpm constant temperature shaker at
149 25 °C. In order to explore the effect of pH on adsorption, 0.1 g P-BC was put into 100 mL IBP
150 solution (2000 μg/L), and the solution pH values were adjusted to 2, 3, 4, 5, 6, 7 and 8,

151 respectively. To explore the effect of dosage on the adsorption, amounts of 0.01, 0.05, 0.10,
152 0.12, 0.15 and 0.20 g P-BC, respectively, were placed into 100 mL IBP solution (2000 μg/L,
153 pH 2). The effect of coexisting ions on adsorption was studied by adding 0.1 g P-BC into 100
154 mL IBP solution (2000 μg/L, pH 2), and then NaCl (0.0584g), $NaNO_3$ (0.0850g), Na_2SO_4
155 (0.1420g) and Na_3PO_4 (0.1639g) were added to the solution, respectively. These steps were
156 repeated and 0.0058, 0.0584 and 0.5844g NaCl were added to the solution, respectively. Since
157 the volume of coexisting ions added were relatively small, the volume of IBP was uniformly
158 calculated with 100 ml for convenience of calculation. The samples after adsorption were taken
159 to determine the IBP concentration.

160 *2.5. Regeneration procedure*

161 P-BC (0.1 g) was added to the 100 mL IBP solution (2000 μg/L, pH 2) and the conical
162 flask was oscillated at 25 ℃ and 150 rpm for 24 h. The adsorbed P-BC was ultrasonically
163 cleaned twice with a small amount of ethanol for 5 min each time. After that, it was washed
164 with deionized water several times and dried in the oven, and then the above regeneration
165 process was repeated 5 times.

166 The solution was filtered with an 0.22 μm organic membrane after adsorption and detected
167 by Ultra Performance Liquid Chromatography (UPLC, SIL-30AC, Japan). A C18 column (3.5
168 μm，2.1×100 mm) and UV-visible detection (wavelength of 220 nm) were selected. Ultrapure
169 water-1% glacial acetic acid: methanol = 3:7 was used as the mobile phase for low-pressure
170 gradient elution with a total flow rate of 0.4 mL/min. Three groups of parallel experiments were
171 operated and the detection results were averaged. The removal efficiency and equilibrium

adsorption capacity of IBP by P-BC were calculated by Eqs. (1) and (2), respectively.

$$R(\%)=\frac{C_0-C_e}{C_0}\times 100\% \quad (1)$$

Where, R is the IBP removal efficiency (%), C_0 is the initial concentration of IBP (μg/L), and C_e is the concentration of IBP at adsorption equilibrium (μg/L).

$$q_e=\frac{C_0-C_e}{m}\times V \quad (2)$$

Where, q_e is the adsorption capacity of P-BC at adsorption equilibrium (μg/g), m is the mass of P-BC (g), and V is the volume of IBP solution (L).

2.6. Adsorption kinetics

The pseudo-first order, pseudo-first order, elovich and intra-particle diffusion kinetic models served to evaluate the adsorption kinetics in this study and calculated by Eqs. (3), (4), (5) and (6), respectively.

Pseudo-first-order: $\ln(q_e-q_t)=\ln q_e-k_1 t$ (3)

Pseudo-second-order: $\frac{t}{q_t}=\frac{1}{k_2 q_e^2}+\frac{t}{q_e}$ (4)

Elovich: $q_t=\left(\frac{1}{b}\right)\ln ab+\left(\frac{1}{b}\right)\ln t, t_0=\frac{1}{ab}$ (5)

Intra-particle diffusion: $q_t=k_i t^{0.5}+C_i$ (6)

Where, q_t (μg/g) is the amount of IBP adsorbed by P-BC at time t (min), q_e is the amount of IBP adsorbed by P-BC at adsorption equilibrium (μg/g), k_1 and k_2 are the rate constants of pseudo-first order kinetics (min^{-1}) and pseudo-second order kinetics ($g\cdot\mu g^{-1}\cdot min^{-1}$), a is the rate constant of chemisorption, b is the constant of the surface coverage, k_i is intra-particle diffusion rate constant ($\mu g\cdot g^{-1}\cdot min^{-0.5}$), and C_i is a constant (μg /g).

192 *2.7. Adsorption isotherm*

193 To further explore the adsorption mechanism of P-BC, the Langmuir, Freundlich, Temkin

194 and Redlich-Peterson models were employed to evaluate the adsorption capacity of P-BC and

195 calculated by Eqs. (7), (8), (9) and (10), respectively.

196 Langmuir: $Q_e=\frac{Q_m K_L C_e}{1+K_L C_e}$ (7)

197 Freundlich: $Q_e=K_F C_e^{1/n}$ (8)

198 Temkin: $Q_e=\left(\frac{RT}{b_T}\right)\ln(K_T C_e)$ (9)

199 Redlich-Peterson: $Q_e=\frac{K_R C_e}{\left(1+a_R C_e^{\beta_R}\right)}$ (10)

200 where, Q_e is the amount of IBP adsorbed by P-BC at adsorption equilibrium (μg/g), Q_m denotes

201 the maximum adsorption capacity of IBP (μg/g), K_L stands for the Langmuir constant (L/μg),

202 and C_e represents the equilibrium concentration of IBP (μg/L), K_F is a constant representing the

203 adsorption capacity of P-BC and *1/n* is a constant indicating the intensity of the adsorption. *R*

204 and b_T are universal gas constant (8.314 $J\cdot mol^{-1}\cdot K^{-1}$) and Temkin constant, *T* is temperature in

205 terms of Kelvin, and K_T is equilibrium bond constant related to the maximum energy of bond,

206 K_R, a_R and β_R are Redlich–Peterson constants and the exponent, β_R, lies between 0 and 1.

207

208 **3. RESULTS AND DISCUSSION**

209 *3.1. Physicochemical properties of P-BC*

210 The yield of P-BC prepared by pyrolysis at 600 °C was 34.3%, and this was probably due

211 to the fact that most of the cellulose and hemicellulose decomposed at higher temperature,

212 resulting in a smaller yield [28]. The elemental composition (i.e., C, H, O, and N) of plane tree

leaves and P-BC are shown in Table 1. P-BC showed an increase in C and a decrease in H, O, and N compared to the original plane tree leaves. The ratios of O/C, H/C, and (N+O)/C were indicators of hydrophilicity, aromaticity, and polarity. While the decreased ratios of O/C, H/C, and (N+O)/C suggested that pyrolysis of plane tree leaves was a process involving less hydrophilicity and polarity. However, aromaticity was increased [29].

Table 1

Physicochemical properties of plane tree leaves and P-BC.

Sample	Ash content (%)	Elemental composition (%)							Specific surface area (m^2/g)	Pore volume (cm^3/g)	Pore diameter (nm)
		C	H	O	N	H/C	O/C	(N+O)/C			
Plane tree leaves	3.74	47.22	10.22	36.55	2.27	0.22	0.77	0.82	-	-	-
P-BC	13.62	72.49	2.13	10.24	1.42	0.03	0.14	0.16	249.09	0.0379	3.92

Based on what can be seen in Fig. 1a and b, the surface of P-BC was rough with an irregular stacking structure and arranged irregular pore structure, which increased the surface adsorption active sites. As can be observed from Fig. 1c and d, some irregular substances were added to

the surface of P-BC, which proved that IBP molecules were adsorbed on this particular surface.

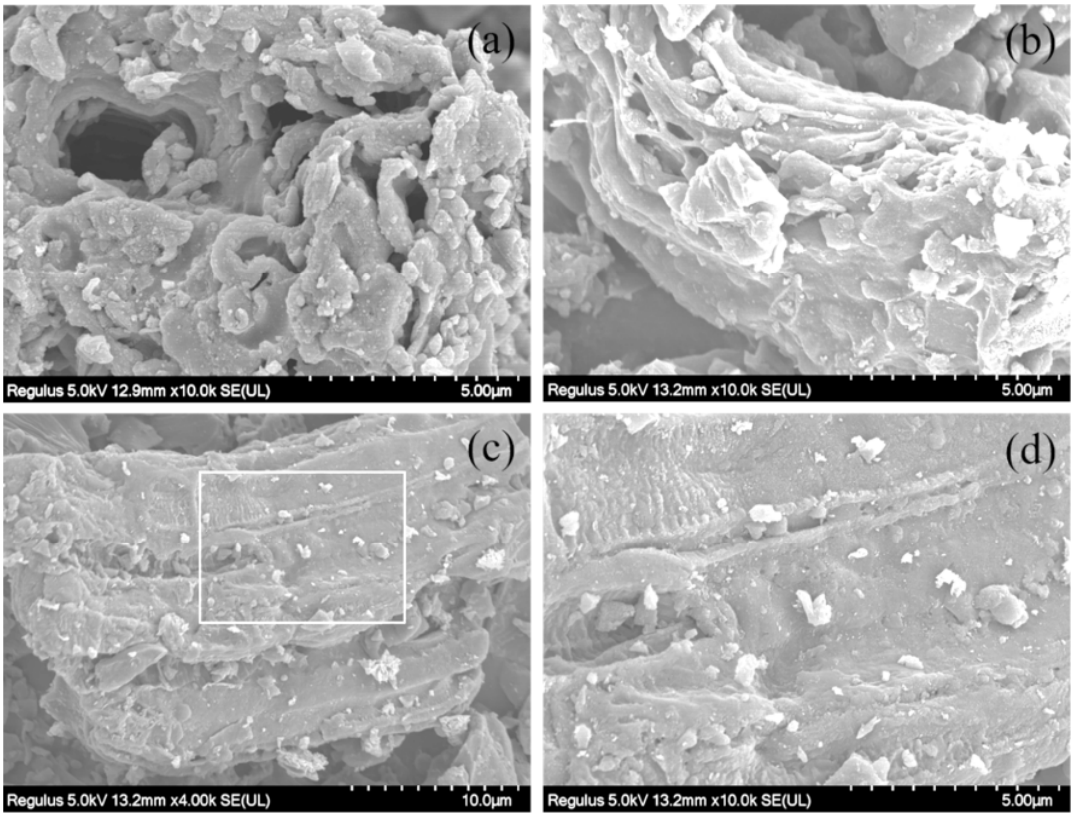

Fig. 1. SEM analysis of P-BC (a, b) before adsorption and (c, d) after adsorption.

The FT-IR spectra of P-BC are shown in Fig. 2, with a broad and sharp peak at 3400 cm^{-1}, indicating that P-BC contains -OH functional groups. The stretching vibration peaks were around: 2800~3000 cm^{-1} as well as 1390 cm^{-1} for saturated C-H; 1630 cm^{-1} for possible C=C; 1000 ~1100 cm^{-1} for possible C-O-C stretching vibration; and 870 cm^{-1} for the v2 absorption peak in calcite crystal, which was related to the bending vibration of C-O bond [19,30]. The -OH absorption vibration peak at 3400 cm^{-1} of P-BC was weakened after adsorbing IBP. The absorption vibration peaks of C-H at 1390 cm^{-1} declined and slightly shifted while the C-O at 880 cm^{-1} also weakened. This consequently indicated that -OH, C-H and C-O played a key role in the adsorption of IBP onto P-BC [31].

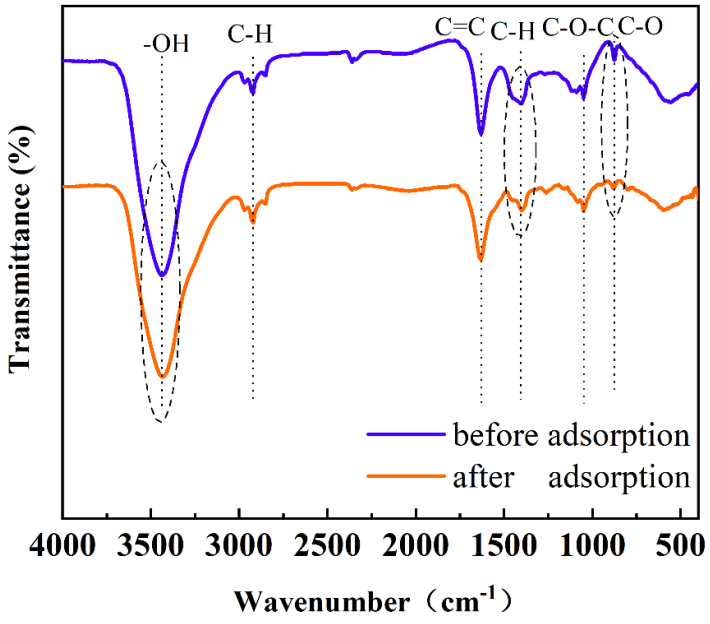

Fig. 2. FTIR analysis of P-BC before and after IBP adsorption.

The surface composition of P-BC before and after IBP adsorption was analyzed by XPS. As can be seen from Fig. 3a, various compositions including C1s, O1s, N1s, and Ca2p emerged through the survey scan of P-BC. The C1s spectra of P-BC were deconvoluted into three peaks at 284.80, 285.74 and 288.63 eV, which were assigned to C-C/C-H (47.59%), C-OH/C-O-C (43.22%) and O-C-O (9.19%), respectively (exhibited in Fig. 3b). After IBP adsorption, the decrease of Ca may be due to chemical adsorption such as metal complexation (see Fig. 3c). Furthermore, the decrease of C-OH/C-O-C after adsorption was contributed as active sites of IBP adsorption (shown in Fig. 3d) [19].

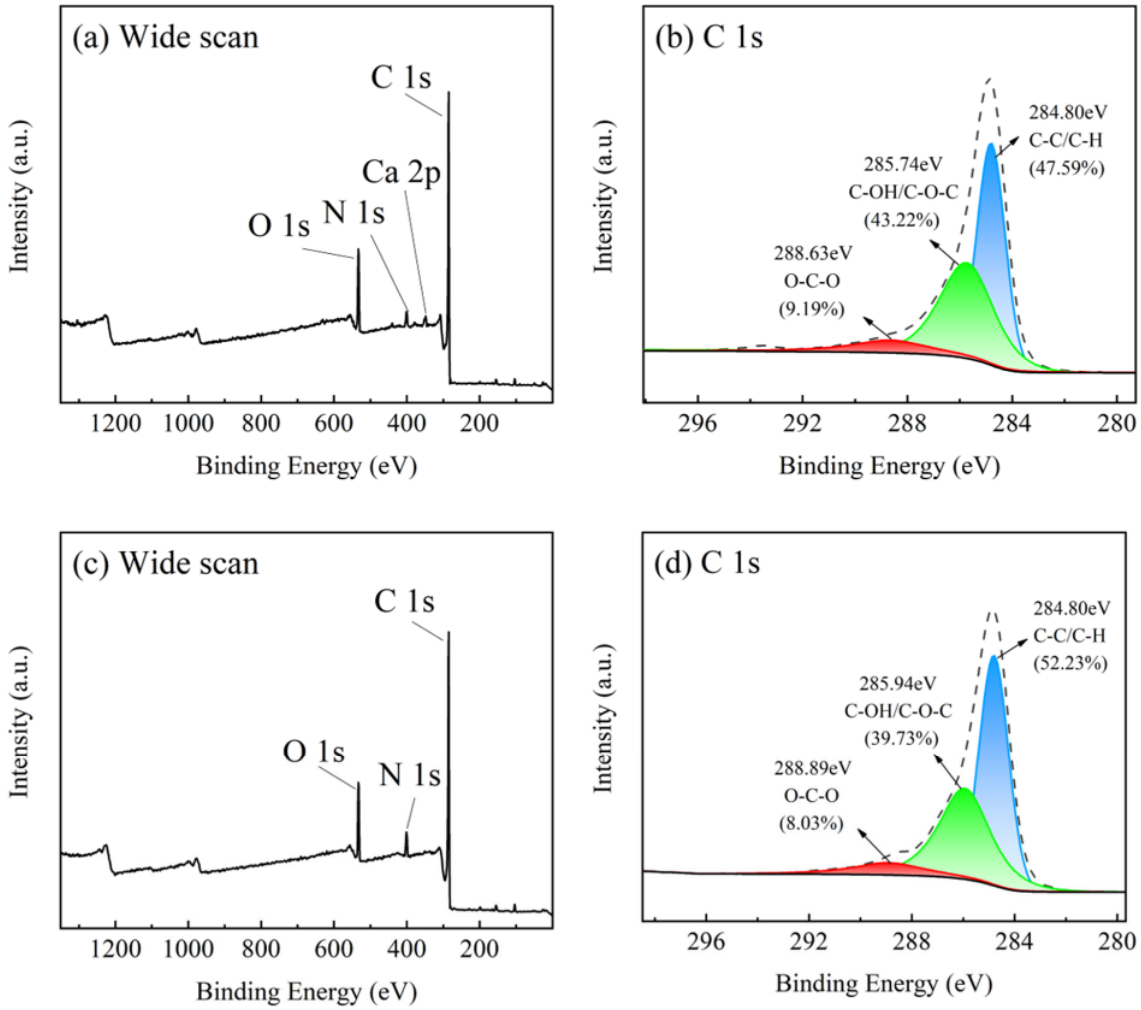

Fig. 3. Wide scan and deconvoluted C 1s XPS spectra of P-BC (a, b) before adsorption and (c, d) after adsorption.

3.2. IBP adsorption by P-BC

3.2.1. Effect of pH on IBP adsorption

The effect of different pH on the adsorption of IBP by P-BC is depicted in Fig. 4a. As can be seen, the removal efficiency of IBP is up to 96.34% at pH 2, and it decreases with the increase of pH. This is due to two factors, pH_{zpc} of P-BC and pK_a of IBP. The pH_{zpc} of P-BC and pK_a of IBP were 3.4 and 4.9, respectively (see Fig. 4b and c). At pH 2, the IBP mainly existed as a molecule, accounting for more than 99 mol%. At pH higher than 4, IBP gradually took on an

anionic form, accounting for 11 mol% and 55 mol% at pH of 4 and 5, respectively. When the pH reached 7, the form of IBP anion was more than 99 mol% [32]. The pH level can affect the chemical morphology of ions presenting in the solution, and alter the charge on the P-BC surface by protonation of surface functional groups. Therefore, as the pH of the solution was less than the pH_{zpc} of P-BC, a positive charge arose on the P-BC surface. Inversely, the P-BC surface developed a negative charge [33]. As a result, under the conditions of pH less than the pK_a of IBP, the nonionized IBP interacted strongly with the P-BC surface [34]. While the pH was larger than the pK_a of IBP, the proportion of IBP existed in the form of carboxylate anions ($R\text{-}COO^-$) and increased gradually. In addition, with the increase of the pH, the electrostatic repulsion between the P-BC surface and carboxylate anions intensified, leading to diminished IBP removal efficiency [21].

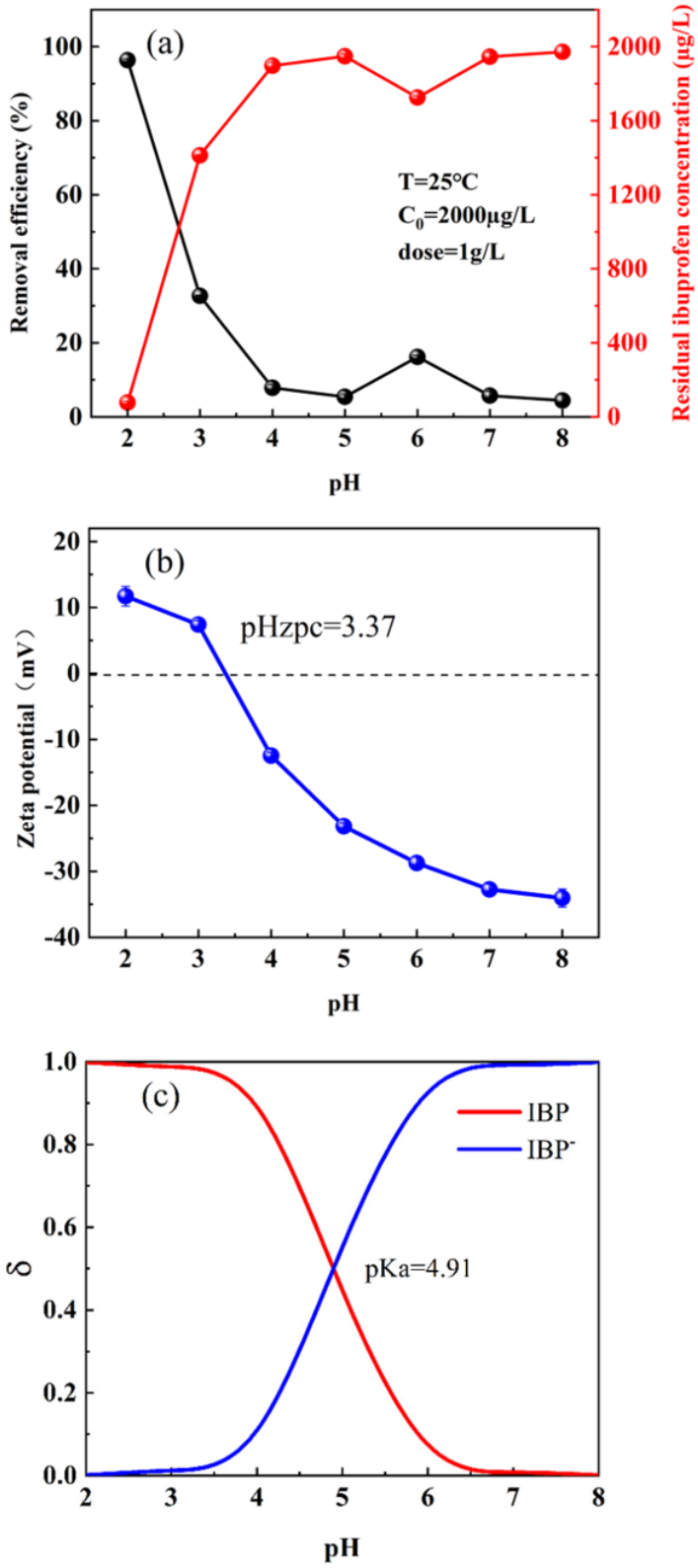

Fig. 4. (a) Effect of solution pH on IBP adsorption (b) Zeta potential analysis of P-BC (c) Distribution function of IBP in water.

273 *3.2.2. Effect of P-BC dosage on IBP adsorption*

274 The effect of adsorbent dosage on IBP adsorption is shown in Fig. S1. When the dosage
275 of P-BC rose from 0.1 g/L to 1.0 g/L, the removal rate of IBP increased rapidly. The removal
276 rate of IBP reached as high as 94.50% at the P-BC dosage of 1.0 g/L. After that, the removal
277 rate of IBP continued to rise slowly as the dose increased, and the IBP was not detected after
278 adsorption when the dosage reached 2.0 g/L. The explanation for this is that with an increase in
279 P-BC dosage, the active sites for adsorbing IBP increased. However, as the dosage continuously
280 increased, the active sites of the adsorbents overlapped, resulting in a large diminishment of
281 adsorption efficiency [23]. Therefore, taking into account the removal efficiency as well as
282 economic issues, a dose of 1.0 g/L was selected as the best possible P-BC dosage for IBP
283 removal.

284 *3.2.3. Effect of coexisting ions on IBP adsorption*

285 There are many salt species in actual wastewater. It contains not only target ions, but also
286 many other coexisting ions, which affect the adsorption capacity of the adsorbent. Therefore,
287 chloride (Cl^-), nitrate (NO_3^-), sulphate (SO_4^{2-}) and phosphate (PO_4^{3-}) (0.01 mol/L) were
288 selected to investigate the effect of coexisting anions on IBP adsorption (see Fig. 5a). The results
289 showed that Cl^- and NO_3^- did not interfere much with the adsorption of IBP by P-BC, and the
290 presence of SO_4^{2-} inhibited the adsorption of IBP. In the presence of PO_4^{3-}, the adsorption
291 capacity of IBP by P-BC dropped to 448 μg/g. This may be due to the pH increase of the solution
292 from 2.0 to 7.9 after the addition of Na_3PO_4, which inhibited IBP adsorption by P-BC due to
293 electrostatic repulsion. The effects of ionic strength on the adsorption of IBP by P-BC were

investigated with NaCl solution of 0.001 mol/L, 0.01 mol/L and 0.1 mol/L. It can be seen from Fig. 5b that NaCl solution promoted the adsorption of IBP by P-BC due to the salting out effect. The coexisting ions competed with IBP for adsorption sites by binding with water molecules, and weakened the hydrogen bond between IBP and water molecules. This led to the decline in IBP solubility in aqueous solution, which was conducive to the diffusion of IBP on the surface of P-BC and increased the adsorption of IBP by P-BC [35].

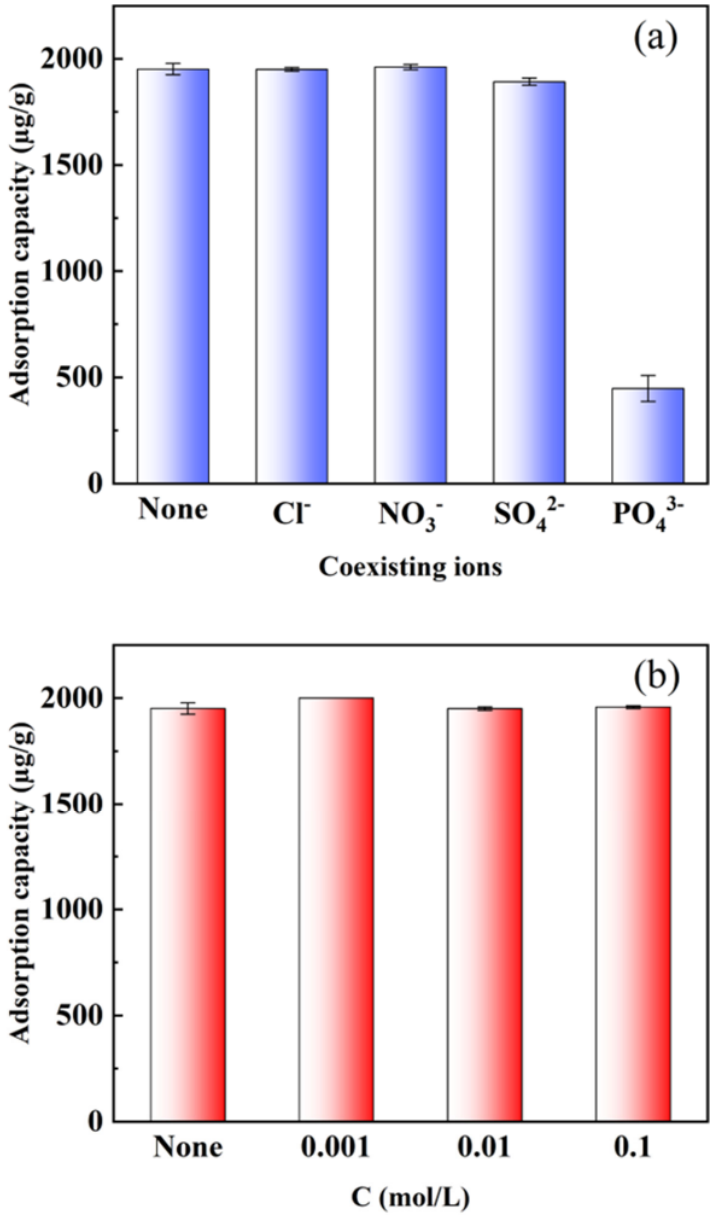

Fig. 5. The effects of different (a) coexisting ions and (b) NaCl concentrations on the adsorption of IBP by P-BC under the conditions of pH = 2, T= 25 °C, C_0=2000 μg/L and P-BC dosage = 1 g/L.

3.3. Adsorption mechanism

The main adsorption mechanism of IBP adsorption by P-BC is shown in Fig. 6. The -OH functional groups on the surface of P-BC could form hydrogen bonds with IBP as donors and acceptors, respectively, which was the main mechanism of IBP adsorption by P-BC. Solution pH played a pivotal role in the adsorption of IBP. When the solution pH was less than the pH_{zpc} of P-BC, the P-BC surface was positively charged. There was, additionally, more H^+ in the solution and the protonated IBP could form electrostatic repulsion with P-BC. However, the hydrogen bonding force between P-BC and IBP was stronger than the electrostatic repulsion and dominated at this point [21,36]. When the solution pH was larger than the pH_{zpc} of P-BC, the acidic groups on the surface of P-BC were ionized and the surface was negatively charged. The proportion of IBP anions increased gradually. At this time, the electrostatic repulsion was dominant, resulting in waning adsorption efficiency. It is worth noting that the phenolic hydroxyl groups on P-BC surface were not ionized at pH 6. They could form hydrogen bonds with IBP and its carboxylate anions, so there was an adsorption peak at pH 6 [21].

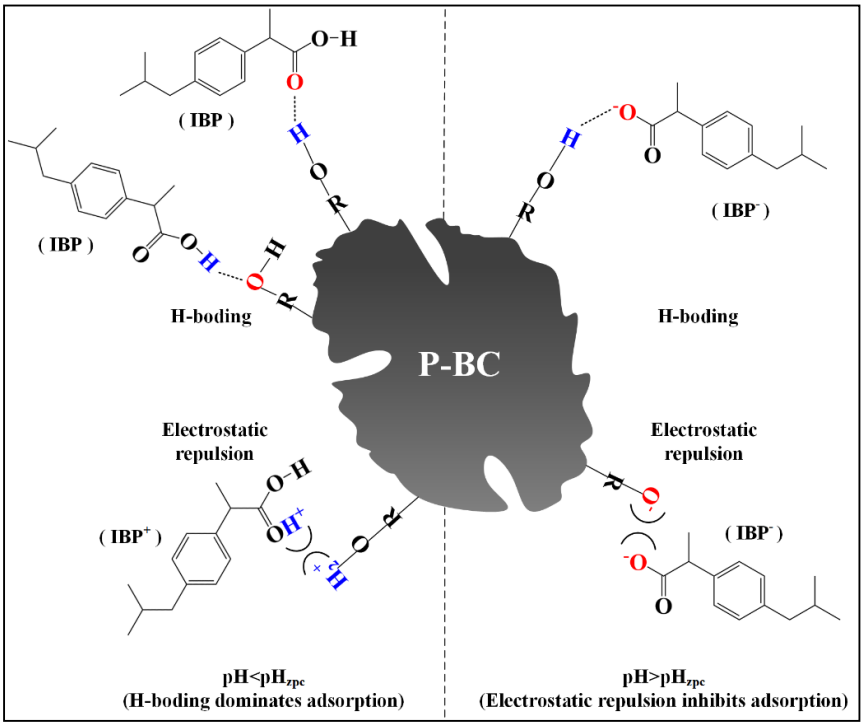

Fig. 6. Adsorption mechanism of IBP by P-BC.

3.4. Adsorption kinetics and isotherm

The kinetic curve fits and parameters of IBP adsorption by P-BC are exhibited in Fig. S2 and Table S1. The pseudo-first order, pseudo-second order, elovich and intra-particle diffusion kinetics models were fitted through the experimental data. As shown here, the adsorption capacity of IBP by P-BC increased with contact time, rapid adsorption occurred in the first 60 min (1 h), and the adsorption reached equilibrium after 1440 min (24 h). The fitting results of intra particle diffusion model indicated that the internal diffusion of adsorbent was not the only control step of adsorption, which may be dominated by surface adsorption and intra particle diffusion [19]. By comparing the fitting results of pseudo first-order, pseudo second-order, elovich and intra particle diffusion kinetic models, the pseudo second-order kinetic model can better describe the adsorption process of IBP by P-BC (R^2=0.999), while the calculated

equilibrium adsorption capacity was very close to the experimental one. This indicated that the adsorption of IBP by P-BC was mainly controlled by chemical adsorption.

The fitting parameters of IBP adsorption isotherm by P-BC are shown in Fig. S3 and Table S2. The Langmuir model is based on the following assumptions: adsorption occurs in a complete monolayer on a homogeneous surface. The Freundlich isotherm is used to describe heterogeneous and reversible multilayer adsorption, and lateral interaction occurs between adsorbed molecules [37]. It was also found that the Langmuir (R^2=0.996) isotherm model could better describe the adsorption of IBP by P-BC. It also showed that monolayer adsorption occurred on the homogeneous surface of P-BC. The adsorption capacity of IBP by P-BC increased when the equilibrium concentration also increased. According to the fitting results of the Langmuir model, the theoretical maximum adsorption capacity of IBP by P-BC was 10410 μg/g. Compared with biochars of other raw materials in Table 2, the adsorption capacity of IBP by P-BC was comparable, and it exhibited several advantages including environmental friendliness, simple preparation, and not requiring any modification.

Table 2

Adsorption capacity of different kinds of biochars for IBP in water.

Raw material	Pyrolysis temperature (°C)	Modifier	Initial concentration (mg/L)	Optimum pH	Adsorption capacity (mg/g)	References
Pine wood	425	-	25~100	3	10.74	[21]
wood apple shell	650	-	3~45	3	5	[23]

Terminalia katappa shell	550	H_3PO_4; NaOH	5~25	2	8.77; 9.52	[24]
Parthenium hysterophorus	500	NaOH	5~100	2	90.46	[32]
Chili seeds	600	-	5~1000	7	26.13	[38]
Plane tree leaves	600	-	0.5~5	2	10.41	This study

348 *3.5. Regeneration of P-BC*

349 Due to the high solubility of IBP in organic solvents, absolute ethanol was used as eluent.
350 As can be seen from Fig. 7, the removal ratios of IBP by five cycles adsorption were 93.42%,
351 93.22%, 89.95%, 72.25%, and 70.32%, respectively. The removal efficiency of IBP employing
352 P-BC declined after five adsorption cycles, but it was nonetheless still at a higher level. This
353 reusability is an advantage of its low cost, improving its application potential.

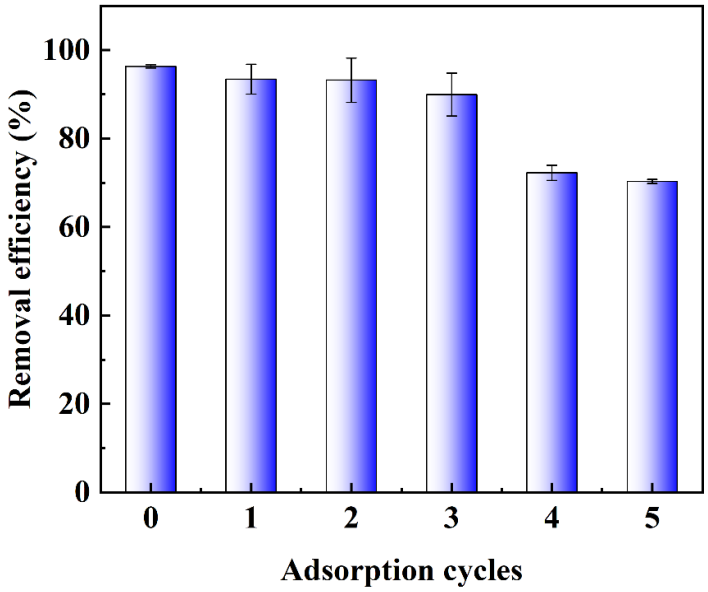

354

355 **Fig. 7.** Cyclic adsorption of IBP by P-BC through absolute ethanol regeneration at pH = 2, T=
356 25 °C, C_0=2000 μg/L and P-BC dosage = 1 g/L.

357 Additionally, although P-BC processed good regeneration, the safe disposal of the

biochar absorbent need to be concerned after repeated recycle use. However, previous studies rarely reported the treatment methods of adsorbents. In consideration of environmental protection, the adsorbent adsorbed with IBP needs to be properly treated, otherwise the pollutants will be released into the environment again. A report issued by the World Health Organization (WHO) put forward the methods of safe disposal of drugs such as waste packaging and incineration, which could safely dispose of used adsorbents [38]. Therefore, inert fixation can be carried out by landfill. Water, cement and lime can be mixed to encapsulate the waste P-BC, and then buried underground.

3.6. Economic feasibility

The production of biochar is proposed based on environmental benefits, but the economic cost remains the key for whether it can have sustained practical applications. Biochar production costs are mainly based on the acquisition costs of raw materials, processing costs and other overhead expenses. The production costs of 1 kg P-BC are shown in Table 3.

Table 3

Estimated costs for producing 1 kg P-BC.

Particulars	Sub sections	Cost analysis	Amount/(USD)
Raw material processing		Free collection from gardens	0
Preparation of	Drying cost	Hours×unit ×per	3.37

biochar from plane tree leaves		unit cost[1]=24×1.8×0.078	
	Carbonization cost	Hours×unit×per unit cost=2×2×0.078	0.312
Other costs		10% of total cost=(3.370+0.312)×10%	0.368
Total cost		3.370+0.312+0.368	4.05

As shown in Table 3, the overall production cost of P-BC is 4.05 USD/kg. Under the best conditions, 1 g/L of P-BC could effectively remove 2000 μg/L of IBP solution, which is equivalent to the treatment cost of only 0.004 USD/L wastewater. According to the research of Show et al. [24], the removal rate of IBP by shell biochar was as high as 92.46%, and the removal cost was 0.012 USD/L without considering regeneration. Compared to it, the cost of removing IBP from water by P-BC in this work is lower. Regenerated by ethanol elution, P-BC could be reused at least five times and the removal rates were all higher than 70%. The regeneration costs were much lower than the production costs, suggesting its potential in practical application.

Currently, the rate of resource utilization for landscaping waste is low and advances in developing it for reuse are few and far between. The lack of a reward mechanism is one of the important reasons for this situation. Due to the risks associated with entrepreneurship and the

[1] per unit cost: cost of electricity per kilowatt-hour.

adoption of new products, government subsidy policies should be seriously considered in order to reduce this problem. Guided by documented economic benefits, giving subsidies and support to enterprises to promote the development of circular bioeconomy using this product must commence as soon as possible [39].

4. CONCLUSIONS

In summary, a low-cost plane tree leaf-derived biochar was prepared by high-temperature pyrolysis at 600 °C. It can efficiently remove ibuprofen from water and realize the utilization of waste as a resource for other processes. P-BC is able to remove a large amount of IBP at 96.34% in acidic conditions, and exhibits the maximum adsorption capacity towards IBP of 10410 μg/g calculated from the Langmuir model. Mechanism analysis verified that the hydrogen bonding interaction was mostly involved in IBP adsorption. P-BC still possessed the ability to adsorb IBP after five regeneration cycles. Overall, P-BC emerges as an environmentally friendly, low-cost, and efficient adsorbent for removing IBP from water, and this study may offer a reference for biomass disposal and resource utilization.

Acknowledgements

This research was supported by Tianjin Municipal Science and Technology Bureau of China (Project No. 18PTZWHZ00140, 20JCZDJC00380) and TG Hilyte Environment Technology (Beijing) Co., LTD. (Project No. M-P-0-181001-001).

References

[1] S. Show, P. Chakraborty, B. Karmakar, and G. Halder, Sorptive and Microbial Riddance of Micro-Pollutant Ibuprofen from Contaminated Water: A State of the Art Review, Sci. Total Environ. 786 (2021) 147327, http://dx.doi.org/10.1016/j.scitotenv.2021.147327.

[2] B. Ren, X. Shi, X. Jin, X. Wang, P. Jin, Comprehensive Evaluation of Pharmaceuticals and Personal Care Products (Ppcps) in Urban Sewers: Degradation, Intermediate Products and Environmental Risk, Chem. Eng. J. 404 (2021) 127024, http://dx.doi.org/10.1016/j.cej.2020.127024.

[3] L. Garcia, J.C. Leyva-Diaz, E. Diaz, S. Ordonez, A Review of the Adsorption-Biological Hybrid Processes for the Abatement of Emerging Pollutants: Removal Efficiencies, Physicochemical Analysis, and Economic Evaluation, Sci. Total Environ. 780 (2021) 146554, http://dx.doi.org/10.1016/j.scitotenv.2021.146554.

[4] M. J. Ahmed, Adsorption of Non-Steroidal Anti-Inflammatory Drugs from Aqueous Solution Using Activated Carbons: Review, J. Environ. Manage. 190 (2017) 274-82, http://dx.doi.org/10.1016/j.jenvman.2016.12.073.

[5] Y. Yang, Y.S. Ok, K.H. Kim, E.E. Kwon and Y.F. Tsang, Occurrences and removal of pharmaceuticals and personal care products (PPCPs) in drinking water and water/sewage treatment plants: A review, Sci. Total Environ. 596-597 (2017) 303-320, http://dx.doi.org/10.1016/j.scitotenv.2017.04.102.

[6] D. Smiljanic, B. de Gennaro, A. Dakovic, B. Galzerano, C. Germinario, F. Izzo, G.E. Rottinghaus, A. Langella, Removal of Non-Steroidal Anti-Inflammatory Drugs from Water by Zeolite-Rich Composites: The Interference of Inorganic Anions on the Ibuprofen

429 and Naproxen Adsorption, J. Environ. Manage. 286 (2021) 112168,
430 http://dx.doi.org/10.1016/j.jenvman.2021.112168.
431 [7] K. Zhang, G. Yuan, A.A. Werdich, Y. Zhao, Ibuprofen and Diclofenac Impair the
432 Cardiovascular Development of Zebrafish (Danio Rerio) at Low Concentrations, Environ.
433 Pollut. 258 (2020) 113613, http://dx.doi.org/10.1016/j.envpol.2019.113613.
434 [8] L. Wang, Y. Peng, X. Nie, B. Pan, P. Ku, S. Bao, Gene Response of Cyp360a, Cyp314, and
435 Gst and Whole-Organism Changes in Daphnia Magna Exposed to Ibuprofen, Comp.
436 Biochem. Physiol. C Toxicol. Pharmacol. 179 (2016) 49-56,
437 http://dx.doi.org/10.1016/j.cbpc.2015.08.010.
438 [9] D.M. Kristensen, C. Desdoits-Lethimonier, B. Jégou, Correction for Kristensen Et Al.,
439 Ibuprofen Alters Human Testicular Physiology to Produce a State of Compensated
440 Hypogonadism, Proc. Natl. Acad. Sci. U.S.A. 115 (2018) E4143,
441 http://dx.doi.org/10.1073/pnas.1805313115.
442 [10] B. Hu, S. Hu, Z. Chen, J. Vymazal, Employ of Arbuscular Mycorrhizal Fungi for
443 Pharmaceuticals Ibuprofen and Diclofenac Removal in Mesocosm-Scale Constructed
444 Wetlands, J. Hazard. Mater. 409 (2021) 124524,
445 http://dx.doi.org/10.1016/j.jhazmat.2020.124524.
446 [11] M. Hasan, K. Alfredo, S. Murthy, R. Riffat, Biodegradation of Salicylic Acid,
447 Acetaminophen and Ibuprofen by Bacteria Collected from a Full-Scale Drinking Water
448 Biofilter, J. Environ. Manage. 295 (2021) 113071,
449 http://dx.doi.org/10.1016/j.jenvman.2021.113071.

450 [12] H. Gong, W. Chu, Y. Huang, L. Xu, M. Chen, M. Yan, Solar Photocatalytic Degradation
451 of Ibuprofen with a Magnetic Catalyst: Effects of Parameters, Efficiency in Effluent,
452 Mechanism and Toxicity Evolution, Environ. Pollut. 276 (2021) 116691,
453 http://dx.doi.org/10.1016/j.envpol.2021.116691.
454 [13] L. Jothinathan, J. Hu, Kinetic Evaluation of Graphene Oxide Based Heterogenous
455 Catalytic Ozonation for the Removal of Ibuprofen, Water Res. 134 (2018) 63-73,
456 http://dx.doi.org/10.1016/j.watres.2018.01.033.
457 [14] R. Ghemit, A. Makhloufi, N. Djebri, A. Flilissa, L. Zerroual, M. Boutahala, Adsorptive
458 Removal of Diclofenac and Ibuprofen from Aqueous Solution by Organobentonites: Study
459 in Single and Binary Systems, Groundw. Sustain. Dev. 8 (2019) 520-529,
460 http://dx.doi.org/10.1016/j.gsd.2019.02.004.
461 [15] R. Davarnejad, B. Soofi, F. Farghadani, and R. Behfar, Ibuprofen Removal from a
462 Medicinal Effluent: A Review on the Various Techniques for Medicinal Effluents
463 Treatment, Environ. Technol. Innov. 11 (2018) 308-320,
464 http://dx.doi.org/10.1016/j.eti.2018.06.011.
465 [16] S.N.F. Ali, E.I. El-Shafey, S. Al-Busafi, H.A.J. Al-Lawati, Adsorption of
466 Chlorpheniramine and Ibuprofen on Surface Functionalized Activated Carbons from
467 Deionized Water and Spiked Hospital Wastewater, J. Environ. Chem. Eng. 7 (2019)
468 102860, http://dx.doi.org/10.1016/j.jece.2018.102860.
469 [17] L. Rafati, M.H. Ehrampoush, A.A. Rafati, M. Mokhtari, A.H. Mahvi, Removal of
470 Ibuprofen from Aqueous Solution by Functionalized Strong Nano-Clay Composite

Adsorbent: Kinetic and Equilibrium Isotherm Studies, Int J Environ Sci Technol. 15 (2017) 513-524, http://dx.doi.org/10.1007/s13762-017-1393-0.

[18] G. Hanbali, S. Jodeh, O. Hamed, R. Bol, B. Khalaf, A. Qdemat, S. Samhan, Enhanced Ibuprofen Adsorption and Desorption on Synthesized Functionalized Magnetic Multiwall Carbon Nanotubes from Aqueous Solution, Materials. 13 (2020), http://dx.doi.org/10.3390/ma13153329.

[19] J. E. Kim, S.K. Bhatia, H.J. Song, E. Yoo, H.J. Jeon, J.Y. Yoon, Y. Yang, R. Gurav, Y.H. Yang, H.J. Kim, Y.K. Choi, Adsorptive Removal of Tetracycline from Aqueous Solution by Maple Leaf-Derived Biochar, Bioresour. Technol. 306 (2020) 123092, http://dx.doi.org/10.1016/j.biortech.2020.123092.

[20] Y. Dai, W. Wang, L. Lu, L. Yan, D. Yu, Utilization of Biochar for the Removal of Nitrogen and Phosphorus, J. Clean. Prod. 257 (2020) 120573, http://dx.doi.org/10.1016/j.jclepro.2020.120573.

[21] M. Essandoh, B. Kunwar, C.U. Pittman, D. Mohan, T. Mlsna, Sorptive Removal of Salicylic Acid and Ibuprofen from Aqueous Solutions Using Pine Wood Fast Pyrolysis Biochar, Chem. Eng. J. 265 (2015) 219-227, http://dx.doi.org/10.1016/j.cej.2014.12.006.

[22] S. Mondal, K. Bobde, K. Aikat, G. Halder, Biosorptive Uptake of Ibuprofen by Steam Activated Biochar Derived from Mung Bean Husk: Equilibrium, Kinetics, Thermodynamics, Modeling and Eco-Toxicological Studies, J. Environ. Manage. 182 (2016) 581-594, http://dx.doi.org/10.1016/j.jenvman.2016.08.018.

[23] P. Chakraborty, S. Banerjee, S. Kumar, S. Sadhukhan, G. Halder, Elucidation of Ibuprofen

492 Uptake Capability of Raw and Steam Activated Biochar of Aegle Marmelos Shell:
493 Isotherm, Kinetics, Thermodynamics and Cost Estimation, Process Saf Environ Prot. 118
494 (2018) 10-23, http://dx.doi.org/10.1016/j.psep.2018.06.015.
495 [24] S. Show, S. Mukherjee, M.S. Devi, B. Karmakar, G. Halder, Linear and Non-Linear
496 Analysis of Ibuprofen Riddance Efficacy by Terminalia Catappa Active Biochar:
497 Equilibrium, Kinetics, Safe Disposal, Reusability and Cost Estimation, Process Saf
498 Environ Prot. 147 (2021) 942-964, http://dx.doi.org/10.1016/j.psep.2021.01.024.
499 [25] L. Cao, G. Luo, D.C.W. Tsang, H. Chen, S. Zhang, J. Chen, A Novel Process for Obtaining
500 High Quality Cellulose Acetate from Green Landscaping Waste, J. Clean. Prod. 176 (2018)
501 338-347, http://dx.doi.org/10.1016/j.jclepro.2017.12.077.
502 [26] T. Yue, D. Jiang, Z. Zhang, Y. Zhang, Y. Li, T. Zhang, Q. Zhang, Recycling of Shrub
503 Landscaping Waste: Exploration of Bio-Hydrogen Production Potential and Optimization
504 of Photo-Fermentation Bio-Hydrogen Production Process, Bioresour. Technol. 331 (2021)
505 125048, http://dx.doi.org/10.1016/j.biortech.2021.125048.
506 [27] X. Hu, X. Zhang, H.H. Ngo, W. Guo, H. Wen, C. Li, Y. Zhang, C. Ma, Comparison study
507 on the ammonium adsorption of the biochars derived from different kinds of fruit peel, Sci.
508 Total Environ. 707 (2020) 135544, https://doi.org/10.1016/j.scitotenv.2019.135544.
509 [28] Y.K. Choi, E. Kan, Effects of Pyrolysis Temperature on the Physicochemical Properties of
510 Alfalfa-Derived Biochar for the Adsorption of Bisphenol a and Sulfamethoxazole in Water,
511 Chemosphere. 218 (2019) 741-748, http://dx.doi.org/10.1016/j.chemosphere.2018.11.151.
512 [29] A.U. Rajapaksha, M. Vithanage, M. Zhang, M. Ahmad, D. Mohan, S.X. Chang, Y.S. Ok,

Pyrolysis Condition Affected Sulfamethazine Sorption by Tea Waste Biochars, Bioresour. Technol. 166 (2014) 303-308, http://dx.doi.org/10.1016/j.biortech.2014.05.029.

[30] X. Zhang, Y. Zhang, H.H. Ngo, W. Guo, H. Wen, D. Zhang, C. Li, L. Qi, Characterization and Sulfonamide Antibiotics Adsorption Capacity of Spent Coffee Grounds Based Biochar and Hydrochar, Sci. Total Environ. 716 (2020) 137015, http://dx.doi.org/10.1016/j.scitotenv.2020.137015.

[31] T. Yang, Y. Xu, Q. Huang, Y. Sun, X. Liang, L. Wang, X. Qin, L. Zhao, Adsorption Characteristics and the Removal Mechanism of Two Novel Fe-Zn Composite Modified Biochar for Cd(Ii) in Water, Bioresour. Technol. 333 (2021) 125078, http://dx.doi.org/10.1016/j.biortech.2021.125078.

[32] S. Mondal, K. Aikat, G. Halder, Biosorptive Uptake of Ibuprofen by Chemically Modified Parthenium Hysterophorus Derived Biochar: Equilibrium, Kinetics, Thermodynamics and Modeling, Ecol. Eng. 92 (2016) 158-172, http://dx.doi.org/10.1016/j.ecoleng.2016.03.022.

[33] P. Chakraborty, S. Show, W.U. Rahman, G. Halder, Linearity and Non-Linearity Analysis of Isotherms and Kinetics for Ibuprofen Remotion Using Superheated Steam and Acid Modified Biochar, Process Saf Environ Prot. 126 (2019) 193-204, http://dx.doi.org/10.1016/j.psep.2019.04.011.

[34] P. Chakraborty, S.D. Singh, I. Gorai, D. Singh, W.U. Rahman, G. Halder, Explication of Physically and Chemically Treated Date Stone Biochar for Sorptive Remotion of Ibuprofen from Aqueous Solution, J. Water Process. Eng. 33 (2020) 101022, http://dx.doi.org/10.1016/j.jwpe.2019.101022.

[35] M.A. Schlautman, S. Yim, E.R. Carraway, J.H. Lee, B.E. Herbert, Testing a Surface Tension-Based Model to Predict the Salting out of Polycyclic Aromatic Hydrocarbons in Model Environmental Solutions, Water Res. 38 (2004) 3331-3339, http://dx.doi.org/10.1016/j.watres.2004.04.031.

[36] P. Chakraborty, S. Show, S. Banerjee, G. Halder, Mechanistic Insight into Sorptive Elimination of Ibuprofen Employing Bi-Directional Activated Biochar from Sugarcane Bagasse: Performance Evaluation and Cost Estimation, J. Environ. Chem. Eng. 6 (2018) 5287-5300, http://dx.doi.org/10.1016/j.jece.2018.08.017.

[37] Y. Tang, M.S. Alam, K.O. Konhauser, D.S. Alessi, S. Xu, W. Tian, Y. Liu, Influence of Pyrolysis Temperature on Production of Digested Sludge Biochar and Its Application for Ammonium Removal from Municipal Wastewater, J. Clean Prod. 209 (2019) 927-936, http://dx.doi.org/10.1016/j.jclepro.2018.10.268.

[38] R. Ocampo-Perez, E. Padilla-Ortega, N.A. Medellin-Castillo, P. Coronado-Oyarvide, C.G. Aguilar-Madera, S.J. Segovia-Sandoval, R. Flores-Ramirez, A. Parra-Marfil, Synthesis of Biochar from Chili Seeds and Its Application to Remove Ibuprofen from Water. Equilibrium and 3D Modeling, Sci. Total Environ. 655 (2019) 1397-1408, http://dx.doi.org/10.1016/j.scitotenv.2018.11.283.

[39] M. Carus, L. Dammer, The Circular Bioeconomy—Concepts, Opportunities, and Limitations, Ind Biotechnol. 14 (2018) 83-91, http://dx.doi.org/10.1089/ind.2018.29121.mca.